Sketch Drawing by NAO Humanoid Robot

Avinash Kumar Singh , Pavan Chakraborty and G.C.Nandi
Robotics and Artificial Intelligence Laboratory
Indian Institute of Information Technology, Allahabad, India.
avinashkumarsingh1986@gmail.com, pavan@iiita.ac.in, gcnandi@iiita.ac.in

***Abstract*—This paper demonstrates the sketch drawing capability of NAO humanoid robot. Two redundant degrees of freedom elbow yaw (RElbowYaw) and wrist yaw (RWristYaw) of the right hand have been sacrificed because of their less contribution in drawing. The Denavit-Hartenberg (DH) parameters of the system has been defined in order to measure the working envelop of the right hand as well as to achieve the inverse kinematic solution. A linear transformation has been used to transform the image points with respect to real world coordinate system and novel 4 point calibration technique has been proposed to calibrate the real world coordinate system with respect to NAO end effector.**

Keywords—NAO calibration, D-H principal, sketch drawing, boundary extraction, transformations.

I. Introduction

NAO is a 58 centimeters tall humanoid robot designed by a French company Aldebaran [1]. Analogous to human physical specifications, NAO has similar kind of sensors as well as physical attributes. If we categorize the NAO sensory specification we can divide it into four parts (a)Vision Sensor: It helps NAO to perceives outer world, to visually detect objects, recognize humans etc.,(b) Inertial Measurement Unit: it tells NAO's actual body position either it is in the standing posting, siting position or in rest position, (c) Touch Sensor: it brings into notice to NAO that some part of its body has been touched, and lastly NAO has (d) Four directional microphone: it enables NAO to localize sound source and to communicate with us. A complete description about each sensor, body joints and links etc. has been depicted in [2]. NAO has 25 degree of freedom (DOF) (Head 2DOF, Arm(each) 5DOF, Pelvis 1DOF, Leg(each) 5DOF, Hand(each) 1DOF) which enables it to do various job very sophistically.

This paper demonstrates the capability of NAO robot in the field of sketch drawing. The first fully automated humanoid system which could be used as a sketch artist was developed in EPFL taking the help of HOAP-2 robot [3]. Robots can draw the sketch of any person who is sitting in front of it. The primitive techniques of face detections, face boundary detection and edge extraction together with trajectory planning were used in this application. The other effort has been made by Srikaew et al. [4] to create artistic portraits using the ISAC robot. The beauty of using ISAC as a sketch artist is due to its soft hands it can mitigate the drawing as fine as humans. They have McKibben artificial muscle which is an excellent actuator while the stereo vision helps it in 3D representation of the object. Paul a robotic handeye system designed by [5] does the aesthetic human face sketching more accurate than all the previous approaches. It has four degrees of freedom with the camera placed at the body. It has an efficient feedback control and facial feature extraction modules.

During the past few years NAO has marked its presence in the vibrant field of robotics as well as social applications [6][7][8]. It has been used in education to assist their supervisor. Robotics Assisted Language Learning (RALL) [6] is such a program designed and developed by Minoo et al. to provide help to junior high school students in learning the Iranian English. They are becoming a good housekeeper, especially for assisting physically disabled persons [7]. Their role in fighting against autism is very appreciable. Their specially designed program for Autism Spectrum Disorder (ASD) children help them in associating interaction with them and to find other ways to deal with [8]. They can play various sports like soccer, tic-tac- toe, etc. Keeping their interest in sports a Robocup [9] is being organized every year. Apart from their applications in the above said fields, there are lots of other unsolved challenges regarding locomotion, localization, image perception and grasping etc. need to be solved.

This paper extends its contribution towards humanoid sketch drawing and elaborates the process of sketch drawing in a step by step manner. We discuss a solution (calibration) which defines the image plane with respect to an NAO end effector. The problem of representing the image points corresponds to NAO end effector is divided over two sub problems. The first problem is to map image points with respect to table coordinate (the place where NAO is supposed to draw sketches) and the second issue is to represent table coordinate system with respect to NAO end effector. The first problem is solved by applying a linear transformation while the second problem has been tackled by applying a proposed four point calibration which is useful in estimating the rotation and translation matrix between two different coordinate systems (between NAO body coordinate and table Coordinate). Once NAO defines each point of image plane with respect to its body coordinate system, the only thing left is to calculate the feasible inverse kinematic solution for NAO Right Hand. The close form inverse kinematic solution for NAO right hand with five degrees of freedom is very difficult to achieve.

It has been seen and analyzed from our previous project writing alphabet by NAO humanoid robot (https://www.youtube.com/watch?v=lS0nk0w9qrk) that only three joints (RShoulderPitch, RShoulderRoll, RElbowRoll) are actively participating in writing while the rest two joints (RElbowYaw and RWristYaw) have less contribution. As writing is one of the kind of sketch drawing. We have

978-1-4799-8641-5/15/$31.00 © 2015 IEEE

sacrificed RElbowYaw and RWristYaw to reduce degree of freedom involved in right hand. After throwing two degrees of freedom, the problem transformed in such a way that we have to solve an inverse kinematic solution for NAO right hand of two link and three DOF, which is very easier to solve as well as to implement.

The paper is constructed as follows. Section II presents the background of NAO robot and its DH specification. Section-III describes the problem definition in the details. In Section IV and V, we discussed the proposed solution and its validity, Section VI concludes the paper with its limitation and future scope.

II. Estimation of NAO Denavit-Hartenberg (DH) Parameters

NAO has five degrees of freedom in his right as well as left hand. The specification of right and left hand, both are same except their joint's angle of rotation [1][2]. Drawing is performed by NAO's right hand therefore; we have only configured the DH parameter table for the NAO right hand. DH principle defines the relation between joints [10]. In order to establish the DH parameter for NAO it is necessary to define the different degrees of freedom associated with each link [10]. Fig. 1 & Fig. 2 briefly describes different joints and their rotation axis.

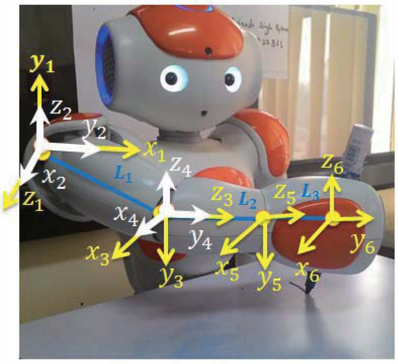

Fig. 1. Coordinate Frame attached on NAO's right hand.

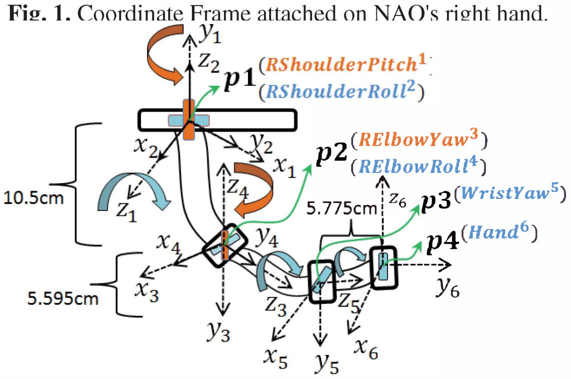

Fig. 2. Sketch representation of NAO's Right hand with axis of rotation and link specifications.

Fig.2 shows the presence of five joints with the help of four symbolic points (p_1, p_2, p_3, p_4). Point p_1 Is located at shoulder having two degrees of freedom Pitch and Yaw. Point p_2 is located at elbow showing the presence of Yaw and Roll while the other two points p_3 and p_4 reflects the rotation along Wrist Yaw and hand. We have added the link length and their axis of rotation additionally for better explanation of the NAO DH parameters. We have used two different colours yellow and white in Fig. 1 and blue and orange in Fig. 2 for symbolizing two different joints at the same place. The DH parameters estimated based on above specification are summarized in Table1.

Table 1. NAO's Right Hand DH parameters for all five joints.

Joint i	Twist angle α_{i-1}	Common Normal a_{i-1}	Offset Length d_i	Joint angle θ_i
1	0	0	0	θ_1
2	-90°	0	0	$\theta_2 - 90$
3	-90°	0	10.50cm	θ_3
4	$+90^\circ$	0	0	θ_4
5	-90°	0	5.595cm	θ_5
6	$+90^\circ$	0	5.775cm	0

The twist angle is measured between Z_i to Z_{i+1}, we have assumed $Z_0$and Z_1 At the same location, therefore the twist angle for first link is set to 0. The other links have their twist angle as $\mp 90^\circ$based on their orientation with respect to frames. The common normal is also set to zero for all links because the z axis of all consecutive links are orthogonal to each other. The link offset is measured along x_{i-1} to x_i. Therefore, it is set to zero for all links that have a common origin. Joint angle is variable because each joint has its own rotation range. The transformation between links $i-1$ *to* i is defined as:

$$T_1^0 = \begin{bmatrix} cos\theta_1 & -sin\theta_1 & 0 & 0 \\ sin\theta_1 & cos\theta_1 & 0 & 0 \\ 0 & 0 & 1 & 0 \\ 0 & 0 & 0 & 1 \end{bmatrix} T_2^1 = \begin{bmatrix} sin\theta_2 & -cos\theta_2 & 0 & 0 \\ 0 & 0 & 1 & 0 \\ -cos\theta_2 & -sin\theta_2 & 0 & 0 \\ 0 & 0 & 0 & 1 \end{bmatrix}$$

$$T_3^2 = \begin{bmatrix} cos\theta_3 & -sin\theta_3 & 0 & 0 \\ 0 & 0 & 1 & l_1 \\ -sin\theta_3 & -cos\theta_3 & 0 & 0 \\ 0 & 0 & 0 & 1 \end{bmatrix} T_4^3 = \begin{bmatrix} cos\theta_4 & -sin\theta_4 & 0 & 0 \\ 0 & 0 & -1 & 0 \\ sin\theta_4 & cos\theta_4 & 0 & 0 \\ 0 & 0 & 0 & 1 \end{bmatrix}$$

$$T_5^4 = \begin{bmatrix} cos\theta_5 & -sin\theta_5 & 0 & 0 \\ 0 & 0 & 1 & l_2 \\ -sin\theta_5 & -cos\theta_5 & 0 & 0 \\ 0 & 0 & 0 & 1 \end{bmatrix} T_6^5 = \begin{bmatrix} 1 & 0 & 0 & 0 \\ 0 & 0 & -1 & -l_3 \\ 0 & 1 & 0 & 0 \\ 0 & 0 & 0 & 1 \end{bmatrix}$$

There are six transformation matrix exists, which are capable to derive the relation between the end effector position with respect to the first link on the right hand. We can define a relation of 6 links to 1st link using the equation (1).

$$T_{endEffector}^{1st\ link} = T_1^0 \times T_2^1 \times T_3^2 \times T_4^3 \times T_5^4 \times T_6^5 \ldots (1)$$

We can further extend it to define the end effector with respect to NAO torso position. In this case the expression will be:

$$T_{endEffector}^{torso} = T_0^{torso} \times T_1^0 \times T_2^1 \times T_3^2 \times T_4^3 \times T_5^4 \times T_6^5 \ldots (2)$$

Where $T_0^{torso}$is defined as:

$$T_0^{torso} = \begin{bmatrix} \cos(90) & -\sin(90) & 0 & 0 \\ \sin(90) & \cos(90) & 0 & -d_1 \\ 0 & 0 & 1 & -d_2 \\ 0 & 0 & 0 & 1 \end{bmatrix}$$

Here d_1 and d_2 are the translation involved along the Y and Z axis from the torso the center point of right hand (p_1). This translation along Y (d_1) Is equal to the sum of SholderOffsetY+ElbowOffsetY, but in the negative direction, similarly the translation along the Z axis (d_2) is equal to the SholderoffsetZ in the negative direction.

The active joints who are participating in sketch drawing are RShoulderPitch, RShoulderRoll, RElbowRoll. The rest two joint joints RElbowYaw and RWristYaw have less contribution in drawing; therefore we have kept these two joints as constant. After losing two degrees of freedom (one along the elbow and one along the wrist), from the right hand, we left with only three degrees of freedom. Keeping the wrist as constant the link length is also reduced to two links (shoulder and wrist combined together and represent one link). The modified coordinate system attached to the NAO right hand is represented in Fig. 3 and its description is presented in Fig. 4. Frames are attached keeping DH principle in mind, which results difference in DH table presented in Table2. The coordinates frames attached in Fig. 3 and Fig. 4 is different from Fig.1 and Fig.2 due to the change in the coordinate axis. The second joint (RShoulderRoll) in the modified coordinate system shown in Fig.3 is parallel to the next joint (RElbowRoll) which enables us to assign the X axis perpendicular to the successive z axis. Link length and their rotation axis are described in Fig. 4. The coordinate system of the last link (fingers) and RElbowRoll has been kept same to reduce the complexity of the system.

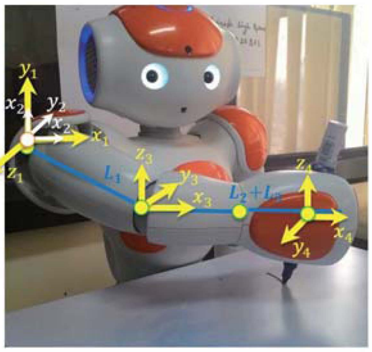

Fig. 3. Coordinate Frame attached on NAO's right hand with only 2 links.

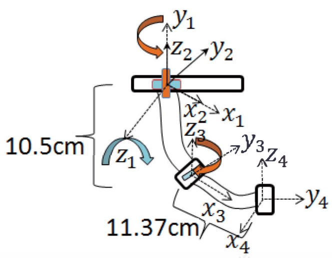

Fig. 4. Specification of modified coordinate system right hand with 2 links.

Table 2. NAO's Right Hand DH parameters for only 3 joints.

Joint i	Twist angle α_{i-1}	Common Normal a_{i-1}	Offset Length d_i	Joint angle θ_i
1	0	0	0	θ_1
2	-90°	0	0	θ_2
3	0	10.50cm	0	θ_3
4	0	11.37cm	0	-90°

The transformation between joint $i-1$ *to* i is reflected in following transformation matrixes. These transformation matrixes are different from the specification due to the removal of two degrees of freedom from the system.

$$T_1^0 = \begin{bmatrix} cos\theta_1 & -sin\theta_1 & 0 & 0 \\ sin\theta_1 & cos\theta_1 & 0 & 0 \\ 0 & 0 & 1 & 0 \\ 0 & 0 & 0 & 1 \end{bmatrix} T_2^1 = \begin{bmatrix} cos\theta_2 & -sin\theta_2 & 0 & 0 \\ 0 & 0 & 1 & 0 \\ -sin\theta_2 & -cos\theta_2 & 0 & 0 \\ 0 & 0 & 0 & 1 \end{bmatrix}$$

$$T_3^2 = \begin{bmatrix} cos\theta_3 & -sin\theta_3 & 0 & 0 \\ sin\theta_3 & cos\theta_3 & 1 & l_1 \\ 0 & 0 & 0 & 0 \\ 0 & 0 & 0 & 1 \end{bmatrix} T_4^3 = \begin{bmatrix} 0 & 1 & 0 & l2 \\ -1 & 0 & 0 & 0 \\ 0 & 0 & 1 & 0 \\ 0 & 0 & 0 & 1 \end{bmatrix}$$

As the modified system has only four transformation matrices. The end effector position with respect to the torso would be defined as:

$$T_{endEffector}^{torso} = T_0^{torso} \times T_1^0 \times T_2^1 \times T_3^2 \times T_4^3 \ldots (3)$$

III. Problem Definition

Given the point $(x_i, y_i)^I$ is corresponding to image plane where $i \in$ imageHeight, $i \in$ imageWidth find out the transformation matrix T such that it will define each point of image plane with respect to NAO end effector position.

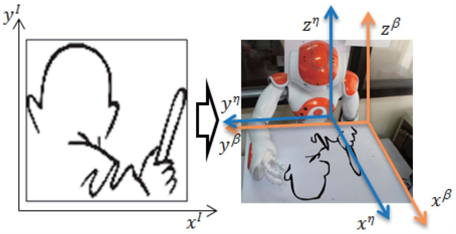

Fig. 5. Problem Definition (Transformation from image plane to NAO end effector position)

The problem is also described in Fig. 5. The first image shows its presence in the image plane later it will be transformed and NAO will perceive it in the form of its end effector position. If $(x', y', z')^{(\eta)}$ are the points corresponding to NAO End effector and $(x, y)^I$ are the points corresponding to Image then the transformation matrix would be:

$$\begin{bmatrix} x' \\ y' \\ z' \end{bmatrix}^\eta = [T] \times \begin{bmatrix} x \\ y \\ 1 \end{bmatrix}^I \ldots (4)$$

The direct transformation from image plane to NAO end effector could be decomposed into two sub problems. First, we can transform the point of the image with respect to table coordinate system (NAO supposed to draw image points on the table) and then we can define the second transformation which we will transform to each point of the table with respect to an NAO end effector. If we introduce the $(x,y,z)^{\beta}$ with respect to table the whole problem will reduce as given below.

$$\begin{bmatrix} x \\ y \\ z \end{bmatrix}^{\beta} = [T_1] \times \begin{bmatrix} x \\ y \\ 1 \end{bmatrix}^{I} \ldots (5) \ \& \ \begin{bmatrix} x' \\ y' \\ z' \\ 1 \end{bmatrix}^{\eta} = [T_2] \times \begin{bmatrix} x \\ y \\ z \\ 1 \end{bmatrix}^{\beta} \ldots (6)$$

IV. PROPOSED SOLUTION

In order to map points from image plane to NAO end effector, it is required to first transform the point with respect to table coordinate and then transform the point in terms of NAO end effector position. In order to do that first we have to physically estimate to what region NAO end effector can reach with respect to the table origin. Once the reachable region's coordinate are retrieved with respect to table origin, the next task is to map every pixel of the image to this reachable region. Let the four reachable corner points defined after the physical measurement of the table with respect to table origin are $(\boldsymbol{x_1}, \boldsymbol{y_1})^{\boldsymbol{\beta}}, (\boldsymbol{x_2}, \boldsymbol{y_2})^{\boldsymbol{\beta}}, (\boldsymbol{x_3}, \boldsymbol{y_3})^{\boldsymbol{\beta}}, (\boldsymbol{x_4}, \boldsymbol{y_4})^{\boldsymbol{\beta}}$. Similarly, we can define the image with four corner points $(\boldsymbol{x_1}, \boldsymbol{y_1})^{\boldsymbol{I}}, (\boldsymbol{x_2}, \boldsymbol{y_2})^{\boldsymbol{I}}, (\boldsymbol{x_3}, \boldsymbol{y_3})^{\boldsymbol{I}}, (\boldsymbol{x_4}, \boldsymbol{y_4})^{\boldsymbol{I}}$. Both image and table's four corners and their mapping are presented in Fig. 6. The z axis of the table have been kept as constant. The relationship between these coordinate systems can be derived with the linear transformation given in equation 7&8.

$$\boldsymbol{\beta_X} = \mathbf{min}(\boldsymbol{\beta_X}) + \frac{\boldsymbol{X}-\mathbf{min}\,(\boldsymbol{I_X})}{\mathbf{max}(\boldsymbol{I_X})-\mathbf{min}\,(\boldsymbol{I_X})} * (\max\,(\boldsymbol{\beta_X})\text{-}\mathbf{min}\,(\boldsymbol{\beta_X})) \ldots (7)$$

$$\beta_Y = \min(\beta_Y) + \frac{Y-\min\,(I_Y)}{\max(I_Y)-\min\,(I_Y)} * (\max\,(\beta_Y)\text{-}\min\,(\beta_Y)) \ldots (8)$$

$$\theta^{\beta} = \{\max(x_1, x_2, x_3, x_4)^{\beta}\}\}, \ominus^{\beta} = \{\min(x_1, x_2, x_3, x_4)^{\beta}\}\},$$

$$\theta^{I} = \{\max(x_1, x_2, x_3, x_4)^{I}\}\}, \ominus^{I} = \{\min(x_1, x_2, x_3, x_4)^{I}\}\}$$

$$\rho^{\beta} = \{\max(y_1, y_2, y_3, y_4)^{\beta}\}\}, \sigma^{\beta} = \{\min(y_1, y_2, y_3, y_4)^{\beta}\}\}$$

$$\rho^{I} = \{\max(y_1, y_2, y_3, y_4)^{I}\}\}, \sigma^{I} = \{\min(x_1, x_2, x_3, x_4)^{I}\}\}$$

$\theta^{\beta}, \ominus^{\beta}, \rho^{\beta}, \sigma^{\beta}$ are the maximum and minimums along the x and y coordinates with respect to table while $\theta^{I}, \ominus^{I}, \rho^{I}, \sigma^{I}$ are the maximum and minimums along the x and y axis with respect to Image coordinate system. A mapping from image plane to table coordinate system is shown in Fig. 5.

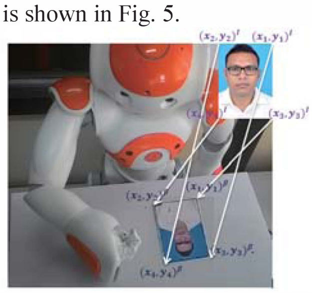

Fig. 6. Image and Board Coordinate System

Here we have taken the input image dimension as 300×300pixel and the reachability physically measured by using NAO with respect to table coordinate is 15×10cm. The image points are extracted from the raw input image with the help of classical canny edge detection [11][12]. The extracted edge points are shown in Fig.7 (b) and the transformed points retrieved after applying the linear transformation as described in Fig.7 (c).

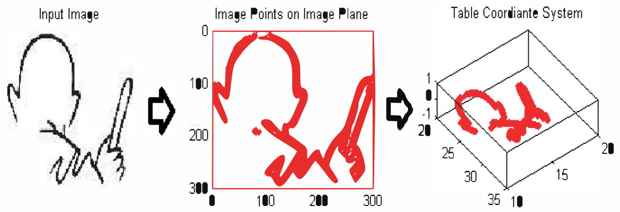

Fig. 7. Transformation from image Plane to board coordinate system (a) Raw Input image (b) Boundary points $(\boldsymbol{x_i}, \boldsymbol{y_i})$extracted with canny edge detection (c) points corresponding to board coordinate system (after transformation)

4.1 *Estimation of Calibration (Homogeneous Transformation) Matrix*

The first step towards solving the inverse kinematic problem for NAO right hand is to establish a relation between the points lies on the Table surface with respect to NAO body coordinate. There are two coordinate system defined in the whole calibration process. One is defined with respect to NAO's torso position symbolized as {N} and second with respect to table symbolized as {T} depicted Fig .8. Both coordinate systems can vary with respect to each other in terms of scaling, translation and rotation. Hence, in order to make a proper alignment with these three parameters should be estimated first. As the Table coordinates and NAO coordinate both are represented in the same unit (meters) we assume that scaling parameter will not play any role here. Hence, it is worthy to estimate only the remaining two parameters.

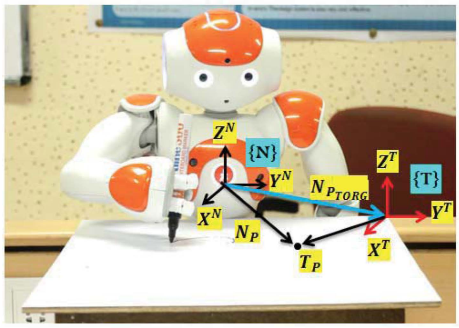

Fig. 8. Image and Table Coordinate System

The calibration matrix which would transform the points from one coordinate frame to another will be made up of rotation and translation parameters. In the given circumstances, this is the simple homogeneous transformation matrix given in equation (9).

$$(x'y'z')^{(\eta)} = H \times (x,y,z)^{\beta} \ldots (9)$$

Where, $(x'y'z')^{(\eta)}$ represents points on the NAO coordinate frame. H is the homogeneous transformation matrix and $(x,y,z)^{\beta}$ are the points represented with respect to Table coordinate frame.

$$\begin{bmatrix} x' \\ y' \\ z' \\ 1 \end{bmatrix} = \begin{bmatrix} f1 & f2 & f3 & f4 \\ f5 & f6 & f7 & f8 \\ f9 & f10 & f11 & f12 \\ 0 & 0 & 0 & 1 \end{bmatrix} \times \begin{bmatrix} x \\ y \\ z \\ 1 \end{bmatrix} \ldots (10)$$

In order to solve the above equation, we have collected four points both from the Table coordinate frame and corresponding points represented with respect to NAO end effector.

4.2 Four Point Calibration

The cost of the transformation presented in equation (10) can be further estimated with the help of 4 point calibration. We need to only have 4 points of table and the corresponding points defined in the NAO's body coordinate system. If we expand the equation (10) we will get following equations.

$$x_i' = f1 * x_i + f2 * y_i + f3 * z_i + f4 \dots (11)$$
$$y_i' = f5 * x_i + f6 * y_i + f7 * z_i + f8 \dots (12)$$
$$z_i' = f9 * x_i + f10 * y_i + f11 * z_i + f12 \dots (13)$$

Here $i \in [1, n]$, n is the number of calibration points (we kept n=4). After expanding equation (11, 12, 13) for all four calibration points, we will get.

$$\begin{bmatrix} x'_1 \\ x'_2 \\ x'_3 \\ \cdot \\ \cdot \\ x'_n \end{bmatrix} = \begin{bmatrix} x_1 & y_1 & z_1 & 1 \\ x_2 & y_2 & z_2 & 1 \\ x_3 & y_3 & z_3 & 1 \\ \cdot & \cdot & \cdot & 1 \\ \cdot & \cdot & \cdot & 1 \\ x_n & y_n & z_n & 1 \end{bmatrix} \times \begin{bmatrix} f1 \\ f2 \\ f3 \\ f4 \end{bmatrix} \dots (14)$$

$$A = T * B$$

If we extend this solution for the rest of the two axes, we will see that the transformation matrix contents are same. This shows that there is no need to estimate the transformation matrix for each independent axis. The four point calibration requires only four points to define the transformation matrix T. The solution of equation (14) can be obtained by simply solving for $B = T^{-1} * A$.

4.2.1 Results obtained after calibration

The beauty of four point calibration is its least number of calibration points. Only four points are sufficient enough to establish the relation between these two coordinate frames. However, the validation of the transformation matrix is being evaluated with the help of two measurement units mean square error and variance depicted in Table3.

Table 3. Statistical Analysis of absolute error involved along each axis.

Measurements (cm)	X Axis	Y Axis	Z Axis
Mean Square Error	0.7087	0.2558	0.0118
Variance	0.1834	0.1069	0.0038

Both measurements shown in Table 3 are calculated on the basis of all 60 samples collected from Table and NAO end effector to test the efficiency of the calibration matrix. The mean square error showed the error involved in projection while the variance shows how the error are distributed along the mean. As Z axis has the mean square error less than other two axes, it has the good projection direction. The absolute error (cm) between the projected samples and the actual sample points is depicted in Fig. 9. It can be seen and analysed from Fig. 9, that in case of projection over Z axis, we have an almost equal amount of error deviation at every point. In other words the deviation is constant for all points which lead to the conclusion that the variance is very low. Hence the transformation along the Z axis is worthy than other two dimensions.

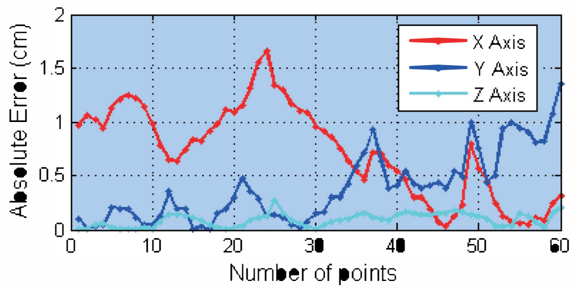

Fig. 9. Absolute error involved along X,Y, Z axis with respect to each sample point

4.3 Inverse kinematics of NAO right hand

After losing two degrees of freedom and combining link2 and link3 into one link, the specification of the right hand has been modified. The updated specification is provided below in Table4.

Table 4. NAO's Right Hand Updated Specifications.

Link	DOF	Range (radian)	Length (cm)
Link 1 (shoulder)	RShoulderPitch	-2.0857 to 2.0857	10.50
Link 1 (shoulder)	RShoulderYaw	-1.3265 to 0.3142	10.50
Link 2 (Elbow)	RElbowRoll	0.0349 to 1.5446	11.37

From the forward kinematic equation (3) of the modified coordinate system defined in section 2, we know the end effector position with respect to NAO torso position is

$$T_{endEffector}^{torso} = T_0^{torso} \times T_1^0 \times T_2^1 \times T_3^2 \times T_4^3$$

Putting all transformation together and solving for $T_{endEffector}^{torso}$ the resultant Cartesian position of the end effector will be:

$$P_x = (l_1 + l_2 c_3)\, c_1 c_2 - l_2\, c_1\, s_2\, s_3 \dots (15)$$
$$P_y = (l_1 + l_2 c_3)\, s_1 c_2 - l_2\, s_1\, s_2\, s_3 \dots (16)$$
$$P_z = -(l_1 + l_2 c_3)\, s_2 - l_2\, c_2\, s_3 \dots (17)$$

where $c_1 = \cos(\theta_1)$, $c_2 = \cos(\theta_2)$, $c_3 = \cos(\theta_3)$ and $s_1 = \sin(\theta_1)$, $s_2 = \sin(\theta_2)$, $s_3 = \sin(\theta_3)$ and l_1, l_2 represents link1 and link 2. Divide equation (16) to equation (15) we will get: $P_y/P_x = s_1/c_1$ then $\tan(\theta_1) = P_y/P_x$ and $\theta_1 = \text{atan}(P_y, P_x)$ Squaring and summing equation (15), (16) and (17) we will get: $P_x^2 + P_y^2 + P_z^2 = l_1^2 + l_2^2 + 2 * l_1 * l_2 * c_3$ Then $c_3 = (P_x^2 + P_y^2 + P_z^2 - l_1^2 - l_2^2)/2 * l_1 * l_2$ and $s_3 = \sqrt{1 - c_3^2}$ and $\theta_3 = \text{atan}(s_3, c_3)$. Let $k_1 = l_1 + l_2 c_3 = \cos\alpha$ and $k_2 = l_2 s_3 = \sin\alpha$, then $\tan(\alpha) = \frac{k_2}{k_1}$ Further, we can conclude; $\alpha = \text{atan}(k_2, k_1)$. Putting the value of k_1 & k_2 into equation (17), we will get;

$$-P_z = \cos\alpha * \sin\theta_2 + \cos\theta_2 * \sin\alpha$$

We also know that; sin (a+b) =sin (a)*cos(b)+cos(a)*sin(b)

Then; $-P_z$=sin $(\theta_2+\alpha)$ and cos $(\theta_2+\alpha)$=$\sqrt{1-{P_z}^2}$

Then; tan$(\theta_2+\alpha)$= $-P_z/\sqrt{1-{P_z}^2}$

Further; $\theta_2+\alpha$=atan$(-P_z,\sqrt{1-{P_z}^2})$

θ_2= atan$(-P_z,\sqrt{1-{P_z}^2})$ –α

After putting the value of α, will be get;

θ_2 = atan2$(-P_z,\sqrt{1-{P_z}^2})$ –atan2(k_2,k_1)

θ_1 = atan2(P_y,P_x) and θ_3=atan(s_3,c_3)

atan2 [13] is used to avoid the ambiguity obtained in solutions.

V. RESULT

We consider the system's absolute error as a prime parameter to validate the system performance. The absolute error is computed between the given trajectory (cartesian space (X,Y,Z)) and the trajectory drawn by the NAO. The given trajectory is computed based on the transformation discussed in section I, while the drawn trajectory is retrieved from the NAO sensor reading. There are different types of functions (api) provided inside the NAO operating system NaoQi, which enables us to read its motor values, position and orientation of each body part such as right hand, left hand, head etc. We draw different category of objects from NAO shown in Fig. 10. The left half of each cell is showing the input image supplied to NAO while the right one is showing the object drawn by NAO. The result are summarized in the form of 9 best drawn objects and their error analysis shown in fig. 11.

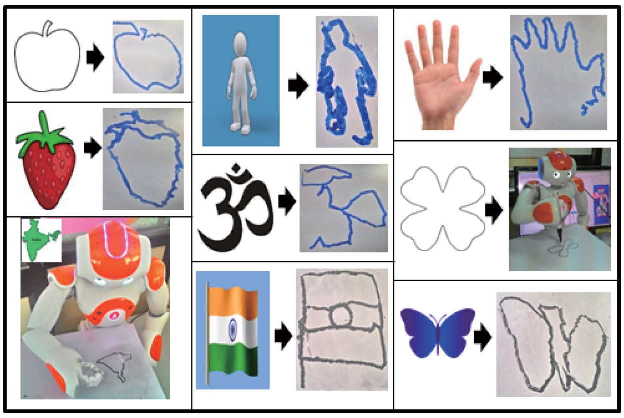

Fig. 10. Top 9 objects drawn by NAO

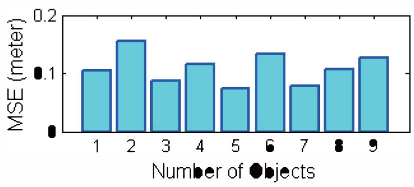

Fig. 11. Mean Square error for each drawn object

Proportional Integral Derivative (PID) controller is used for each joint which feedbacks the error computed between the set point and the measured point [1]. Therefore we receive a smooth drawing trajectory.

VI. CONCLUSION

Two major challenges involved in drawing by NAO robot has been discussed in this paper. These challenges consist of (a) Defining image points with respect to NAO end effector and (b) providing the inverse kinematics solution for NAO right hand. The first problem has been solved by applying the linear interpolation between the image plane and the table coordinate system. The Z axis of the table have been kept as constant to make the mapping linear. Further, these table points are transformed with the help of homogeneous transformation (calibration) matrix in terms on NAO end effector. Two statistical matrices mean square error and variance has been used to measure the quality of transformation. The inverse kinematics problem has been solved by lowering the degrees of freedom from the right hand. Two degrees of freedom along the elbow and wrist have been omitted due to their less contribution in the drawing. Primitive techniques have been used to define image geometrical features which could be improved to get better results in future projects.

REFERENCES

[1] Gouaillier, David, et al. "Mechatronic design of NAO humanoid." *Robotics and Automation, 2009. ICRA'09. IEEE International Conference on*. IEEE, 2009.

[2] Robotics, Aldebaran. "NAO Datasheet H25—Corporate—Aldebaran Robotics| Discover NAO." (2012).

[3] Calinon, Sylvain, Julien Epiney, and Aude Billard. "A humanoid robot drawing human portraits." *Humanoid Robots, 2005 5th IEEE-RAS International Conference on*. IEEE, 2005.

[4] Srikaew, A., et al. "Humanoid drawing robot." IASTED International Conference on Robotics and Manufacturing. 1998.

[5] Tresset, Patrick, and Frederic Fol Leymarie. "Portrait drawing by Paul the robot." *Computers & Graphics* 37.5 (2013): 348-363.

[6] Alemi, Minoo, Ali Meghdari, and Maryam Ghazisaedy. "Employing Humanoid Robots for Teaching English Language in Iranian Junior High-Schools." *International Journal of Humanoid Robotics* 11.03 (2014).

[7] Brown, S. (2014). Meet Pepper, The Emotion Reading Robot. *TECHNOLOGY*.

[8] Shamsuddin, Syamimi, et al. "Initial response of autistic children in human-robot interaction therapy with humanoid robot NAO." *Signal Processing and its Applications (CSPA), 2012 IEEE 8th International Colloquium on*. IEEE, 2012.

[9] Kitano, Hiroaki, et al. "Robocup: The robot world cup initiative." *Proceedings of the first international conference on Autonomous agents*. ACM, 1997.

[10] Craig, John J. *Introduction to robotics: mechanics and control*. Vol. 3. Upper Saddle River: Pearson Prentice Hall, 2005.

[11] Canny, John. "A computational approach to edge detection." *Pattern Analysis and Machine Intelligence, IEEE Transactions on* 6 (1986): 679-698.

[12] Suzuki, Satoshi. "Topological structural analysis of digitized binary images by border following." *Computer Vision, Graphics, and Image Processing* 30.1 (1985): 32-46.

[13] Description of atan2, source: "https://en.wikipedia.org/wiki/Atan2".

[14] Avinash Kumar Singh, G.C Nandi, "Face recognition using facial symmetry", proceedings of the 2nd ACM International Conference on Computational Science, Engineering and Information Technology (CCSEIT-2012), Coimbatore, pp. 550-554, October, 2012.